Table II. Relationship among CT density, arterial remodeling, and the adherent calcium morphology of NCALs

	NCALs with PR (n = 98)	NCALs without PR (n =104)	P*
CT density (HU)			
NCALs	25 ± 23	56 ± 28	<.001
Reference site	351 ± 65	346 ± 65	NS
Adherent calcium morphology (n [%])			
Absence	17 (18)	45 (44)	<.001
Diffuse	9 (9)	21 (20)	.03
Medium	14 (14)	15 (14)	NS
Spotty	58 (59)	23 (22)	<.001

	Adherent calcium morphology				
	Absence (n = 62)	Diffuse (n =30)	Medium (n = 29)	Spotty (n = 81)	P†
CT density (HU)					
NCALs	56 ± 30	57 ± 28	40 ± 25	25 ± 24	<.001
Reference site	345 ± 65	333 ± 66	353 ± 69	355 ± 63	NS
Remodeling index	1.00 ± 0.17	1.03 ± 0.19	1.08 ± 0.18	1.15 ± 0.19	<.001

Data are expressed as mean ± SD or number (percentage) of NCALs. *NS*, Nonsignificant.
*Statistical significance was based on unpaired *t* test or χ^2 test.
†Statistical significance was based on the analysis of variance.

Findings of NCALs detected by MSCT

A total of 202 NCALs were detected in 97 patients (70%, mean 2.1, range 1-5 lesions per patient), whereas no coronary atherosclerotic lesions or only calcified coronary lesions were detected in the remaining 41 patients. The distributions of NCALs were 19 in the left main trunk, 74 in the left anterior descending artery, 29 in the left circumflex artery, and 80 in the right coronary artery. One hundred forty-seven NCALs (73%) were assessed nonobstructive (<50% stenosis) as detected by MSCT angiography. Excellent interobserver agreements were found for the CT densities of NCALs ($r = 0.87$) and reference site lumens ($r = 0.95$).

The numbers of small and large NCALs were 137 and 65, respectively; NCALs with PR (n = 98) had a higher rate of large size than those without PR (n = 104) (43% vs 22%, $P = .002$). A summary of the relationships among CT density, arterial remodeling, and the adherent calcium morphology of NCALs is shown in Table II. The mean CT density of the NCAL with PR was significantly lower than that of the NCAL without PR (25 ± 23 vs 56 ± 28 HU, $P < .001$), and the CT density had a significant inverse correlation with RI ($r = -0.52$, $P < .001$). There was no difference in the mean CT density of the reference site lumen between the PR and non-PR lesions. Noncalcified coronary atherosclerotic lesions with PR were more frequently associated with spotty calcium than those without PR (59 vs 22%, $P < .001$), whereas NCALs without PR were more frequently associated with diffuse calcium or absence of adherent calcium than those with PR. Otherwise, the mean CT density of NCALs with absence of adherent calcium or with diffuse calcium was higher than that of others, whereas that of NCALs with spotty calcium was lower than that of others (absence 56 ± 30, diffuse 57 ± 28, medium 40 ± 25, spotty 25 ± 24 HU, $P < .001$). There was no difference in the mean CT density of the reference site lumen among the 4 adherent calcium groups. The mean RI of NCALs with spotty calcium was largest among the 4 adherent calcium groups (absence

Figure 2

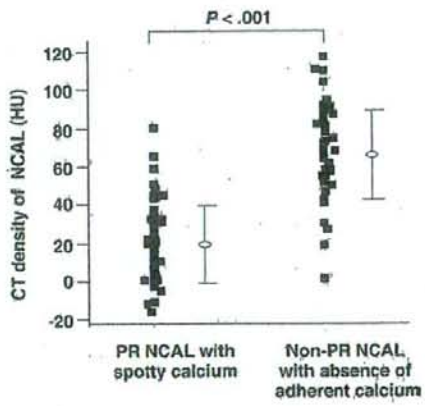

Comparison of CT densities between the PR NCALs with spotty calcium (20 ± 20 HU, n = 58) and non-PR NCALs with absence of adherent calcium (67 ± 24 HU, n = 45) ($P < .001$).

Figure 3

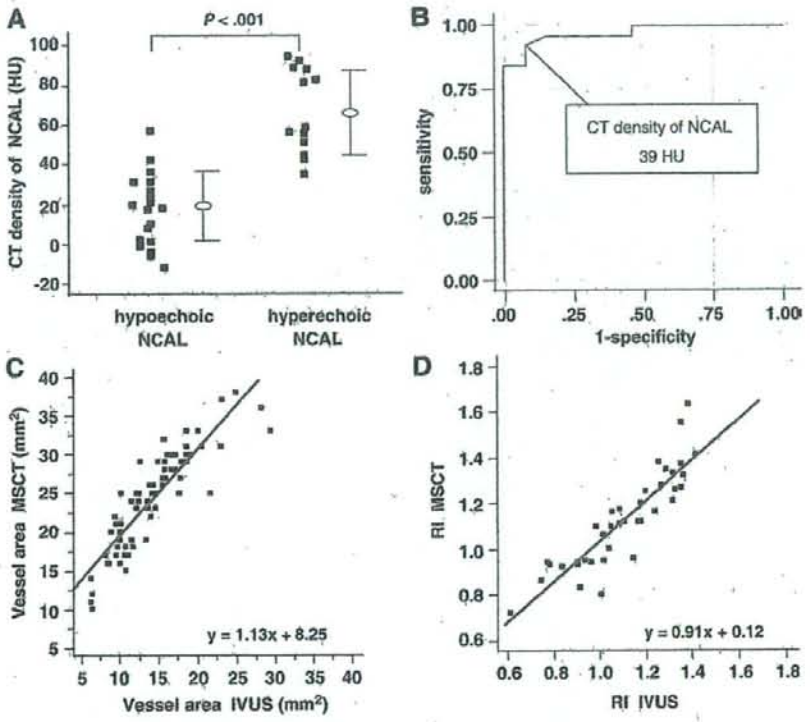

A, Comparison of CT densities between hypoechoic (18 ± 17 HU, n = 25) and hyperechoic NCALs on IVUS (67 ± 21 HU, n =13) ($P < .001$). **B**, Receiver operating characteristic curve analysis of CT density of NCALs for predicting hypoechoic NCALs. **C**, Correlation of cross-sectional vessel areas between IVUS and MSCT (n = 76). **D**, Correlation of RI between IVUS and MSCT (n = 38).

1.00 ± 0.17, diffuse 1.03 ± 0.19, medium 1.08 ± 0.18, spotty 1.15 ± 0.19, $P < .001$).

There was a substantial difference in the mean CT density between the PR lesions with spotty calcium (n = 58) and non-PR lesions with absence of adherent calcium (n = 45) (20 ± 20 vs 67 ± 24 HU, $P < .001$) (Figure 2), whereas there was no difference in the mean CT density of the reference site lumen between the 2 groups.

Comparison of NCAL findings between MSCT and IVUS

The findings of 38 NCALs in the 21 patients were compared between MSCT and IVUS. The mean CT density of hypoechoic lesions (n = 25) was significantly lower than that of hyperechoic lesions (n = 13) (18 ± 17 vs 67 ± 21 HU, $P < .001$), and the optimal cutoff point of CT density for predicting hypoechoic NCALs was 39 HU with a sensitivity of 92% and specificity of 92% (area under the curve 0.97) (Figure 3, *A* and *B*). There was no difference in the mean CT density of the reference site between hypoechoic and hyperechoic lesions on IVUS. Cross-sectional vessel areas measured with MSCT were significantly larger than those measured with IVUS (n = 76, $r = 0.88$, MSCT-IVUS = 10.3 ± 3.1 mm^2, $P < .001$). Otherwise, RI measured with MSCT closely correlated to those measured with IVUS (n = 38, $r = 0.88$, $P < .001$)

Table III. Consensus table of IVUS and 64-slice CT to classify the adherent calcium morphology of NCALs

	IVUS			
64-Slice CT	**No calcium**	**Spotty**	**Intermediate**	**Extensive**
Absence	7	1	0	0
Spotty	0	12	2	0
Medium	0	1	4	2
Diffuse	0	0	3	6

Data are expressed as the number of NCALs.

Figure 4

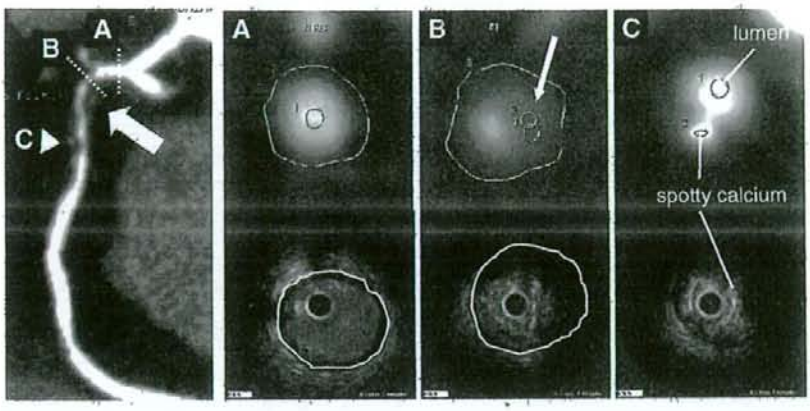

Curved multiplanar reconstruction image showing NCALs (large arrow) in the proximal portion of the right coronary artery. **A**, The cross-sectional vessel areas of the reference site are 25 and 14.0 mm^2 in MSCT and IVUS, respectively. **B**, The cross-sectional vessel areas of the NCALs are 30 and 16.4 mm^2 in MSCT and IVUS, respectively. Therefore, RIs are 1.2 and 1.17 in MSCT and IVUS, respectively. The minimum CT density of the NCAL is 22 HU (small arrow), and IVUS reveals a hypoechoic lesion with echo attenuation. **C**, Both images reveal spotty calcium contained in the NCAL.

(Figure 3, *C* and *D*), and Bland-Altman analysis showed a mean difference of 0.026 ± 0.10, which was not statistically different from zero. The coronary calcium morphology with NCALs evaluated by MSCT gave close agreement with that evaluated by IVUS (Table III). The CT densities of all NCALs with medium or diffuse calcium that were shown as hypoechoic on IVUS were below our optimal cutoff point (8 lesions, median 25, range 1-36 HU). Figure 4 shows a representative case in which the NCAL findings in MSCT are consistent with those in IVUS.

Discussion

To the best of our knowledge, the present study is the first to report the relationship among CT density, vessel enlargement, and the adherent calcium morphology of NCALs detected by 64-slice CT and to demonstrate that lower CT density, PR, and adherent spotty calcium, which may indicate the NCAL vulnerability, are intimately co-related. Our results raise the possibility that these factors regarding NCAL vulnerability may work synergistically in increasing the risk of the occurrence of ACS. We also demonstrate the high reliability of NCAL findings in 64-slice CT imaging compared to IVUS.

Assessment of NCAL vulnerability with MSCT

In a histopathologic study using postmortem hearts, Varnava et al[4] revealed that coronary plaques with PR had a higher lipid content and macrophage count. In another histopathologic study, coronary arterial expansion was strongly correlated with plaque components such as calcium deposits, macrophage infiltrates, and lipid core formation.[18] In line with these previous studies, the present study confirms that NCALs with PR have lower CT densities (which indicates lipid-rich plaques) than those without PR. This finding can be explained by the fact that lipid-rich material may be more prone to enlarge in response to an increase in plaque-wall shear stress.[19]

Ehara et al[6] reported in their IVUS study that the culprit lesions of acute myocardial infarction were frequently characterized by small calcium deposits, associated with a fibrofatty plaque and PR. In human coronary lesion analysis undertaken to test the impact of vessel calcium on biomechanical stresses in atherosclerotic lesions, calcium does not appear to decrease the mechanical stability of the coronary atheroma.[20] We demonstrated that CT densities of NCALs with spotty calcium were low, which suggested that the important factor in the instability of NCALs with spotty calcium might be lipid-rich components. Taking the above into consideration, we assume that NCALs with both PR and spotty calcium, whose CT densities are even lower, may be related to the most unstable stage during the development of coronary atherosclerosis (Stary IV/Va).[21]

The present study also demonstrated that non-PR NCALs were more likely to be associated with the absence of adherent calcium than PR NCALs, and that non-PR NCALs with absence of adherent calcium showed even higher CT densities, indicating lipid-poor plaques. We consider that this type of NCAL may be related to very

early stages with less extracellular lipid accumulation during the development of coronary atherosclerosis (Stary I/II), and which are at low risk for ACS.

A previous ultrasound study revealed that a large arc of calcium is identified as an independent negative predictor of PR.[22] Our results also showed that severe calcium deposits were related to small RI and high CT density. We consider that this type of NCAL may be related to the constrictive remodeling stage with a fibrous increasing component (Stary Vb/Vc); this is likely to be the result of repetitive plaque rupture and healing, causing shrinkage of the vessel.[2]

Reliability of MSCT in comparison to IVUS

Several previous studies have described that the CT densities of coronary plaques measured by 4-slice or 16-slice CT are related to the plaque components evaluated by IVUS.[7,12] The present study demonstrates that 64-slice CT permits a reliable analysis of NCALs regarding the component, arterial remodeling, and adherent calcium morphology, in good correlation with IVUS. Our data showed that cross-sectional vessel areas measured with MSCT were larger than those measured with IVUS. One of the reasons for this discrepancy is the difference in the measured areas between the 2 modalities: in MSCT measurements, we traced the outer vessel contour that was considered as vessel adventitia, whereas in IVUS measurements, the external elastic membrane was used. The other reason is the partial volume effects that occur at the border of the vessel/surrounding pericardial tissue in MSCT images; however, we consider the usefulness of 64-slice CT comparable to that of IVUS in the evaluation of arterial remodeling.

Study limitations

Beam hardening caused by severe calcium may be likely to increase the CT densities of NCALs; however, our CT density measurements of lesions that were hypoechoic in IVUS images were highly reliable despite the presence of severe calcium. Otherwise, contrast density within coronary lumen may influence on the density values measured within plaques. In the present study, although the comparisons of contrast densities within the coronary lumens (reference sites) showed no significant difference between or among the respective groups, a method having smaller differences in coronary lumen contrast among lesions is required to compare the CT density more exactly. Coronary plaque enhancement during contrast injection has also been reported in a recent study.[23] More precise density measurements that reflect the NCAL components in CT angiography require further investigation. The exclusion of lesions with >120 HU from NCALs may introduce bias because there may be subsets of unstable lesions with smaller lipid core and greater calcification. For improvements in coronary plaque characterization using MSCT, a dual-energy scanning is expected to improve temporal resolution, whereas an automated imaging system for classification of normal tissues in medical images obtained from CT scans is expected to enable clearer evaluation of the vessel wall.[24,25]

In comparing MSCT and IVUS findings, the methods used in determining the adherent coronary calcium morphology differ: for MSCT this was determined based on both the width and length of the calcium burden, whereas in IVUS, only the cross-sectional arc of the calcium burden was used.

The present study was retrospectively designed and contained no patients with acute myocardial infarction. A prospective study that includes these patients is required to establish a noninvasive method for detecting rupture-prone coronary plaques and high-risk patients.

Finally, the relatively high-radiation dose of 64-slice CT should be emphasized. At present, CT angiography for coronary plaque imaging alone could not be recommended.

Conclusions

Our data demonstrate that 64-slice CT enables a reliable analysis of NCALs compared to IVUS, and that lower CT density, PR, and adherent spotty calcium, which may indicate the NCAL vulnerability, are intimately co-related. Our results agree with previous histopathologic and IVUS findings regarding coronary plaques and may indicate that these features of NCALs work synergistically in increasing the risk of the occurrence of ACS. Noninvasive and comprehensive analysis of NCALs with 64-slice CT may be useful to detect vulnerable coronary lesions and "vulnerable patients" at risk for ACS.

References

1. Falk E, Shah PK, Fuster V. Coronary plaque disruption. Circulation 1995;92:657-71.
2. Virmani R, Kolodgie FD, Burke AP, et al. Lessons from sudden coronary death: a comprehensive morphological classification scheme for atherosclerotic lesions. Arterioscler Thromb Vasc Biol 2000;20:1262-75.
3. Kolodgie FD, Burke AP, Frab A, et al. The thin-cap fibroatheroma: a type of vulnerable plaque: the major precursor lesion to acute coronary syndromes. Curr Opin Cardiol 2001;16:285-92.
4. Varnava AM, Mills PG, Davies MJ. Relationship between coronary artery remodeling and plaque vulnerability. Circulation 2002;105:939-43.
5. Schoenhagen P, Ziada KM, Kapadia SR, et al. Extent and direction of arterial remodeling in stable versus unstable coronary syndromes. An intravascular ultrasound study. Circulation 2000;101:598-603.
6. Ehara S, Kobayashi Y, Yoshiyama M, et al. Spotty calcification typifies the culprit plaque in patients with acute myocardial infarction. Circulation 2004;110:3424-9.
7. Schroeder S, Kopp AF, Baumbach A, et al. Noninvasive detection and evaluation of atherosclerotic coronary plaques with multislice computed tomography. J Am Coll Cardiol 2001;37:1430-5.

8. Hausleiter J, Meyer T, Hadamitzky M, et al. Prevalence of noncalcified coronary plaques by 64-slice computed tomography in patients with an intermediate risk for significant coronary artery disease. J Am Coll Cardiol 2006;46:312-8.
9. Butler J, Shapiro M, Reiber J, et al. Extent and distribution of coronary artery disease: a comparative study of invasive versus noninvasive angiography with computed tomography. Am Heart J 2007;153: 378-84.
10. Komatsu S, Hirayama A, Omori Y, et al. Detection of coronary plaque by computed tomography with a novel plaque analysis system, 'Plaque Map', and comparison with intravascular ultrasound and angioscopy. Circ J 2005;69:72-7.
11. Nikolaou K, Becker CR, Muders M, et al. Multidetector-row computed tomography and magnetic resonance imaging of atherosclerotic lesions in human ex vivo coronary arteries. Atherosclerosis 2004;174:243-52.
12. Leber A, Knez A, Becker A, et al. Accuracy of multidetector spiral computed tomography in identifying and differentiating the composition of coronary atherosclerotic plaques: a comparative study with intracoronary ultrasound. J Am Coll Cardiol 2004;43:1241-7.
13. Achenbach S, Ropers D, Hoffmann U, et al. Assessment of coronary remodeling in stenotic and nonstenotic coronary atherosclerotic lesions by multidetector spiral computed tomography. J Am Coll Cardiol 2004;43:842-7.
14. Morin RL, Gerber TC, McCollough CH. Radiation dose in computed tomography of the heart. Circulation 2003;107:917-22.
15. Mollet NR, Cademartiri F, Nieman K, et al. Noninvasive assessment of coronary plaque burden using multislice computed tomography. Am J Cardiol 2005;95:1165-9.
16. Kajinami K, Seki H, Takekoshi N, et al. Coronary calcification and coronary atherosclerosis: site by site comparative morphologic study of electron beam computed tomography and coronary angiography. J Am Coll Cardiol 1997;29:1549-56.
17. Mintz GS, Nissen SE, Anderson WD, et al. American College of Cardiology clinical expert consensus document on standards for acquisition, measurement and reporting of intravascular ultrasound studies (IVUS): a report of the American College of Cardiology Task Force on Clinical Expert Consensus Documents. J Am Coll Cardiol 2001;37:1478-92.
18. Burke AP, Kolodgie FD, Farb A, et al. Morphological predictors of arterial remodeling in coronary atherosclerosis. Circulation 2002; 105:297-303.
19. Lafont A, Guzman LA, Whitlow PL, et al. Restenosis after experimental angioplasty: intimal, medial and adventitial changes associated with constrictive remodeling. Circ Res 1995;76:996-1002.
20. Huang H, Virmani R, Younis H, et al. The impact of calcification on the biomechanical stability of atherosclerotic plaques. Circulation 2001; 103:1051-6.
21. Stary HC, Chandler AB, Dinsmore RE, et al. A definition of atherosclerotic lesions and a histological classification of atherosclerosis. Circulation 1995;92:1355-74.
22. Sabate M, Kay IP, de Feyter PJ, et al. Remodeling of atherosclerotic coronary arteries varies in relation to location and composition of plaque. Am J Cardiol 1999;84:135-40.
23. Halliburton SS, Schoenhagen P, Nair A, et al. Contrast enhancement of coronary atherosclerotic plaque: a high-resolution, multidetector-row computed tomography study of pressure-perfused, human ex-vivo coronary arteries. Coron Artery Dis 2006;17: 553-60.
24. Achenbach S, Ropers D, Kuettner A, et al. Contrast-enhanced coronary artery visualization by dual-source computed tomography—initial experience. Eur J Radiol 2006;57:331-5.
25. Dettori L, Semler L. A comparison of wavelet, ridgelet, and curvelet-based texture classification algorithms in computed tomography. Comput Biol Med 2007;37:486-98.

JACC: CARDIOVASCULAR IMAGING
© 2009 BY THE AMERICAN COLLEGE OF CARDIOLOGY FOUNDATION
PUBLISHED BY ELSEVIER INC.

VOL. 2, NO. 2, 2009
ISSN 1936-878X/09/$36.00
DOI:10.1016/j.jcmg.2008.09.015

Characterization of Noncalcified Coronary Plaques and Identification of Culprit Lesions in Patients With Acute Coronary Syndrome by 64-Slice Computed Tomography

Toshiro Kitagawa, MD,* Hideya Yamamoto, MD, FACC,* Jun Horiguchi, MD,‡ Norihiko Ohhashi, MD,* Futoshi Tadehara, MD,* Tomoki Shokawa, MD,* Yoshihiro Dohi, MD,* Eiji Kunita, MD,* Hiroto Utsunomiya, MD,* Nobuoki Kohno, MD,† Yasuki Kihara, MD, FACC*

Hiroshima, Japan

OBJECTIVES We sought to characterize noncalcified coronary atherosclerotic plaques in culprit and remote coronary atherosclerotic lesions in patients with acute coronary syndrome (ACS) with 64-slice computed tomography (CT).

BACKGROUND Lower CT density, positive remodeling, and adjacent spotty coronary calcium are characteristic vessel changes in unstable coronary plaques.

METHODS Of 147 consecutive patients who underwent contrast-enhanced 64-slice CT examination for coronary artery visualization, 101 (ACS; n = 21, non-ACS; n = 80) having 228 noncalcified coronary atherosclerotic plaques (NCPs) were studied. Each NCP detected within the vessel wall was evaluated by determining minimum CT density, vascular remodeling index (RI), and morphology of adjacent calcium deposits.

RESULTS The CT visualized more NCPs in ACS patients (65 lesions, 3.1 ± 1.2/patient) than in non-ACS patients (163 lesions, 2.0 ± 1.1/patient). Minimum CT density (24 ± 22 vs. 42 ± 29 Hounsfield units [HU], $p < 0.01$), RI (1.14 ± 0.18 vs. 1.08 ± 0.19, $p = 0.02$), and frequency of adjacent spotty calcium of NCPs (60% vs. 38%, $p < 0.01$) were significantly different between ACS and non-ACS patients. Frequency of NCPs with minimum CT density <40 HU, RI >1.05, and adjacent spotty calcium was approximately 2-fold higher in the ACS group than in the non-ACS group (43% vs. 22%, $p < 0.01$). In the ACS group, only RI was significantly different between 21 culprit and 44 nonculprit lesions (1.26 ± 0.16 vs. 1.09 ± 0.17, $p < 0.01$), and a larger RI (≥1.23) was independently related to the culprit lesions (odds ratio: 12.3; 95% confidential interval: 2.9 to 68.7, $p < 0.01$), but there was a substantial overlap of the distribution of RI values in these 2 groups of lesions.

CONCLUSIONS Sixty-four-slice CT angiography demonstrates a higher prevalence of NCPs with vulnerable characteristics in patients with ACS as compared with stable clinical presentation. (J Am Coll Cardiol Img 2009;2:153–60) © 2009 by the American College of Cardiology Foundation

From the Departments of *Cardiovascular Medicine, and †Molecular and Internal Medicine, Graduate School of Biomedical Sciences, Hiroshima University, Hiroshima, Japan; and the ‡Department of Clinical Radiology, Hiroshima University Hospital, Hiroshima, Japan.

Manuscript received August 19, 2008; revised manuscript received September 16, 2008, accepted September 24, 2008.

JACC: CARDIOVASCULAR IMAGING, VOL. 2, NO. 2, 2009
FEBRUARY 2009:153–60

The recently developed technology of multidetector computed tomography (MDCT) has the potential to noninvasively identify and characterize noncalcified coronary atherosclerotic plaques (NCPs) in vivo (1,2). A potentially interesting application would be the identification of patients or individual coronary lesions with an increased likelihood of plaque rupture or erosion, leading to acute coronary events. Some previous studies have identified plaque characteristics typically observed by computed tomography (CT) in patients with acute coronary syndrome (ACS). Such characteristics included lower CT density, positive remodeling (PR), and adjacent spotty calcium deposits (3,4). We previously reported that, in comparison with intravascular ultrasound (IVUS), 64-slice CT allows reliable analysis of the components, vascular remodeling, and adjacent calcium morphology of NCPs and could document that lower CT density, PR, and adjacent spotty coronary calcium frequently co-existed in potentially "vulnerable" lesions (5). We consequently hypothesize that these morphologic factors of NCPs might act synergistically to increase the risk of ACS.

See page 161

ABBREVIATIONS AND ACRONYMS

ACS = acute coronary syndrome
CT = computed tomography
ECG = electrocardiogram
HU = Hounsfield units
IVUS = intravascular ultrasound
MDCT = multidetector computed tomography
NCP = noncalcified coronary atherosclerotic plaque
NSTEMI = non–ST-segment elevation myocardial infarction
PR = positive remodeling
RI = remodeling index

Although most previous analyses were limited to culprit lesions in ACS patients (3,4), we designed the study reported here to characterize all NCPs—including nonculprit lesions—in patients with ACS with 64-slice CT. We also compared the NCP characteristics in patients with ACS with others with stable coronary artery disease.

METHODS

Study patients. From November 2006 to October 2007, we enrolled 147 consecutive patients with proven or suspected coronary artery disease (96 men and 51 women, 67 ± 11 years), who underwent MDCT angiography for follow-up or diagnosis of coronary artery disease. Exclusion criteria for MDCT angiography included cardiac arrhythmias (i.e., atrial fibrillation or frequent paroxysmal premature beats), contraindications for iodinated contrast medium, unstable hemodynamic conditions, and ST-segment elevation myocardial infarction. Furthermore, patients with previous ACS, percutaneous coronary intervention, and/or coronary artery bypass grafting were excluded. The study was approved by our hospital's ethical committee, and written informed consent was obtained from all patients.

We assigned patients to the ACS (non–ST-segment elevation myocardial infarction [NSTEMI] and unstable angina) or the non-ACS group according to standard criteria (6). Specifically, NSTEMI was defined as a new finding of ST-segment depression of >0.1 mm or T-wave inversion of at least 0.3 mm in more than 2 anatomically contiguous leads and elevation of troponin-I levels (>0.05 ng/ml). Unstable angina was defined as a new onset of severe, progressive, or resting angina without elevation of electrocardiographic (ECG) ST-segment and troponin-I level. Patients without any of these criteria and with stable clinical presentation (equivocal or positive cardiac stress test, atypical chest pain, or stable exertional chest pain) were assigned to the non-ACS group.

For all patients in the ACS group, invasive coronary angiography was performed within 24 h after MDCT angiography. Vessel narrowing was measured with quantitative coronary angiography analysis (QCA-CMS, Version 5.3, MEDIS Medical Imaging Systems, Leiden, the Netherlands) in the projection that revealed the highest degree of stenosis, and obstructive stenosis was defined as luminal diameter narrowing >50% compared with the reference site. Per patient, 1 single obstructive coronary stenosis was identified as the culprit lesion. When multiple obstructive coronary stenoses were detected, the culprit lesion was defined as the lesion whose appearance was associated with ECG changes or as the lesion with the most obstructive luminal narrowing.

MDCT scan protocol and reconstruction. MDCT angiography was performed with a 64-slice CT scanner (LightSpeed VCT, GE Healthcare, Waukesha, Wisconsin; gantry rotation time, 0.35 s; 64 × 0.625 mm detector collimation, retrospective ECG gating). Patients with a resting heart rate ≥60 beats/min received 40 mg metoprolol orally 60 min before MDCT scanning; all received 0.3 mg nitroglycerin sublingually just before scanning. Our scan protocol and reconstruction methods have been described previously (5). In brief, after a plain scan to determine the calcium burden of the coronary tree and measure coronary calcium score according to the standard Agatston method (sequential scan with 16 × 2.5 mm collimation; tube current 140 mA; tube voltage 120 kV), we acquired a contrast-enhanced data set 30 to 50 ml (0.6 to 0.7 ml/kg) contrast medium (Iopamidol, 370 mg I/ml, Bayer Healthcare, Berlin, Germany) during an inspiratory

breath-hold. The volume data set was acquired in helical mode (64 × 0.625 mm collimation; CT pitch factor, 0.18 to 0.24:1; tube current, 600 to 750 mA with ECG-correlated tube current modulation; tube voltage, 120 kV). The effective radiation dose was estimated on the basis of the dose-length product and ranged from 15 to 18 mSv (5). Image reconstruction was performed with image-analysis software (CardIQ, GE Healthcare) on a dedicated computer workstation (Advantage Workstation Ver.4.2, GE Healthcare). A "standard" kernel was used as the reconstruction filter. Depending on heart rate, either a half-scan (temporal window = 175 ms) or multi-segment (temporal window <175 ms) reconstruction algorithm was selected, and the optimal cardiac phase with the least motion artifacts was chosen individually.

Evaluation of NCP characteristics. All coronary segments >2 mm in diameter were evaluated by 2 blinded and independent observers with curved multiplanar reconstructions and cross-sectional images rendered perpendicular to the vessel center line. The definitions of NCPs and coronary calcium were as follows (5): NCP: a low-density mass >1 mm^2 in size, located within the vessel wall and clearly distinguishable from the contrast-enhanced coronary lumen and the surrounding pericardial tissue; coronary calcium: a structure on the vessel wall with a CT density above that of the contrast-enhanced coronary lumen or with a CT density of >120 Hounsfield units (HU) assigned to the coronary artery wall in a plain image. For NCPs and calcium analyses, the optimal image display setting was chosen on an individual basis; in general, the window was between 700 and 1,000 HU, and the level between 100 and 200 HU.

As previously described (5), we determined the minimum CT density in each NCP by placing at least 5 regions of interest (area = 1 mm^2) in each lesion and documenting the lowest average value of all regions of interest, and on the basis of our previous results (5), low-density NCPs were defined as lesions with a minimum CT density of <40 HU. We also determined the extent of luminal enhancement of each coronary lesion by placing a region of interest (area = 1 mm^2) in the center of the coronary artery lumen at the respective reference segment. On the basis of measurements of the cross-sectional vessel areas (mm^2) at each NCP site of maximum vessel area and each proximal reference site of the same coronary artery, we calculated the "Remodeling Index" (RI). Positive remodeling was defined as RI >1.05 (7). Finally, we assessed calcium deposits in or adjacent to each NCP by determining their presence or absence and their morphology. Spotty calcium was defined as follows: length of calcium burden <3/2 of vessel diameter and width <2/3 of vessel diameter (8). If the initial classification of NCP and adjacent calcium differed among the 2 independent observers, final classification was achieved by consensus.

Statistical analysis. Coronary calcium score is expressed as median value and range, and other measurements are expressed as mean ± SD. Continuous and categorical variables were compared with the Mann-Whitney test and chi-square test, respectively. Interobserver variability of measured CT densities and cross-sectional vessel areas was determined by calculating Pearson's correlation coefficient. In comparisons between ACS and non-ACS lesions and culprit and nonculprit lesions, we used only lesion specific factors, not including patient characteristics because lesions clustered in a single patient. Parameters of NCPs were tested with a receiver-operator characteristic curve to assess their reliability as prognostic variables for predicting ACS culprit lesions. Logistic regression was used to examine the associations between NCP characteristics (RI, presence of adjacent spotty calcium, NCP CT density, and reference site CT density) and ACS culprit lesions for multivariate analysis adjusted for the location of NCPs. All analyses were done with JMP 5.0.1 statistical software (SAS Institute Inc., Cary, North Carolina). A p value of <0.05 was considered statistically significant.

RESULTS

Baseline characteristics. The mean heart rate during scanning was 61 ± 10 beats/min; mean scan time for coronary CT angiography was 6.3 ± 2.1 s. No patient experienced any complication due to MDCT, and no patient was excluded from analysis due to poor image quality of the 64-slice CT.

Of the 147 patients, 46 (31%) had no NCPs as detected by 64-slice CT angiography (31 patients had no coronary atherosclerotic lesions, and 15 patients had only calcified coronary lesions), and all 46 had presented with stable symptoms. In the remaining 101 patients (69%) (21 patients with ACS [8 NSTEMI and 13 unstable anginas] and 80 of 126 patients with stable clinical presentation [non-ACS: no symptom, atypical chest pain, or stable exertional chest pain]), CT angiography allowed detection of at least 1 coronary lesion that contained noncalcified components. A total of 228 NCPs were visualized (on average, 2.2 ± 1.2/patient; range, 1 to 5 lesions/patient). Clinical

Table 1. Patients' Characteristics

	ACS Group (n = 21)	Non-ACS Group (n = 80)	p Value
Age (yrs)	66 ± 11	69 ± 9	NS
Male/female	17/4	61/19	NS
Hypertension	13 (62)	53 (66)	NS
Hyperlipidemia	12 (57)	37 (46)	NS
Diabetes mellitus	8 (38)	39 (49)	NS
Previous or current smoker	12 (57)	45 (56)	NS
Statin use	8 (38)	23 (29)	NS
Heart rate (beats/min)	59 ± 7	59 ± 9	NS
Body mass index (kg/m²)	25 ± 3	24 ± 4	NS
Coronary calcium score	184 (0–1,550)	107 (0–4,656)	NS

N = 101. Coronary calcium score is expressed as median value (range). Other data are the mean value ± SD or n (%) of patients.
ACS = acute coronary syndrome.

characteristics of the 101 patients with NCPs are shown in Table 1. There were no statistically significant differences between ACS and non-ACS groups. Figure 1 shows MDCT and invasive angiographic findings in a case with ACS.

Comparisons of NCP findings between ACS and non-ACS patients. Sixty-five and 163 NCPs were detected in the ACS (n = 21) and non-ACS (n = 80) group, respectively. The location of NCPs in the ACS and non-ACS groups was similar (6% and 10% in the left main coronary artery, 37% and 39% in the left anterior descending artery, 20% and 15% in the left circumflex artery, 37% and 36% in the right coronary artery, respectively). The mean number of NCPs/patient was significantly higher in the ACS group (3.1 ± 1.2) than in the non-ACS group (2.0 ± 1.1, $p < 0.01$). Comparisons of NCP characteristics between the 2 groups are shown in Table 2. Excellent inter-observer agreement was found for minimum CT densities of NCPs ($r = 0.91$), for luminal densities at the reference site lumens ($r = 0.94$), and for all cross-sectional vessel areas ($r = 0.88$). The minimum CT density of NCPs was significantly lower in the ACS group (24 ± 22 HU) than in the non-ACS group (42 ± 29 HU, $p < 0.01$). There was no difference in mean CT densities of reference site lumens between the ACS and non-ACS groups. The mean RI of NCPs was significantly higher in the ACS group than in the non-ACS group (1.14 ± 0.18 vs. 1.08 ± 0.19, $p = 0.02$). Noncalcified coronary atherosclerotic plaques were more frequently associated with spotty calcification in the ACS group (60%) as compared with the non-ACS group (38%, $p < 0.01$). Furthermore, the frequency of low-density NCPs with PR and spotty calcium was substantially higher in the ACS group (43%) than in the non-ACS group (22%, $p < 0.01$).

CT characteristics of culprit versus nonculprit lesions in ACS patients. In the 21 ACS patients, 21 culprit and 44 nonculprit NCPs were detected. Of these lesions, 32 (21 culprit and 11 nonculprit) were assessed as obstructive (>50% stenosis) by invasive angiography. Comparisons of NCP characteristics between culprit and nonculprit lesions in the ACS group are shown in Table 3. The frequency of adjacent spotty calcium was similar in both types of plaques (57% vs. 61%). The minimum CT density of the culprit lesions tended to be lower than that of the nonculprit lesions (15 ± 13 HU vs. 28 ± 24 HU), but this difference did not reach statistical significance. The mean RI of the culprit lesions (1.26 ± 0.16) was significantly higher than that of the nonculprit lesions (1.09 ± 0,17, $p < 0.01$), but there was a substantial overlap of the distribution of RI values in these 2 groups of lesions (Fig. 2). The optimal cutoff for RI by CT angiography to predict culprit lesions was 1.23 and had a sensitivity of 71% and specificity of 82% (area under the curve 0.77). The frequency of plaques that displayed all 3 parameters of "vulnerability" (low CT density, positive remodeling, and spotty calcium) tended to be higher for culprit lesions (57%) compared with nonculprit lesions (36%). However, the difference was not significant. Multivariate analysis, which included larger RI (≥1.23), the presence of adjacent spotty calcium, the minimum NCP CT density, and the reference site CT density, revealed that a larger RI was the only significant predictor of ACS culprit lesions (odds ratio: 12.3; 95% confidence interval: 2.9 to 68.7, $p < 0.01$). Furthermore, the mean RI of the 21 culprit lesions was significantly higher than that of the 11 obstructive nonculprit lesions (1.26 ± 0.16 vs. 1.08 ± 0.16, $p < 0.01$), whereas the minimum CT densities (15 ± 13 HU vs. 15 ± 18 HU), frequencies of adjacent spotty calcium (57% vs. 64%), and frequencies of low-density NCPs with PR and spotty calcium (57% vs. 45%) were similar.

DISCUSSION

In this study, we demonstrated that 64-slice CT coronary angiography allows visualization of more noncalcified coronary atherosclerotic lesions with characteristics assumed to be associated with plaque "vulnerability" in patients with ACS as compared with patients with stable clinical presentation. Thus, 64-slice CT might contribute toward the differentiation of "vulnerable patients." Furthermore, we observed that a high degree of positive remodeling is the most

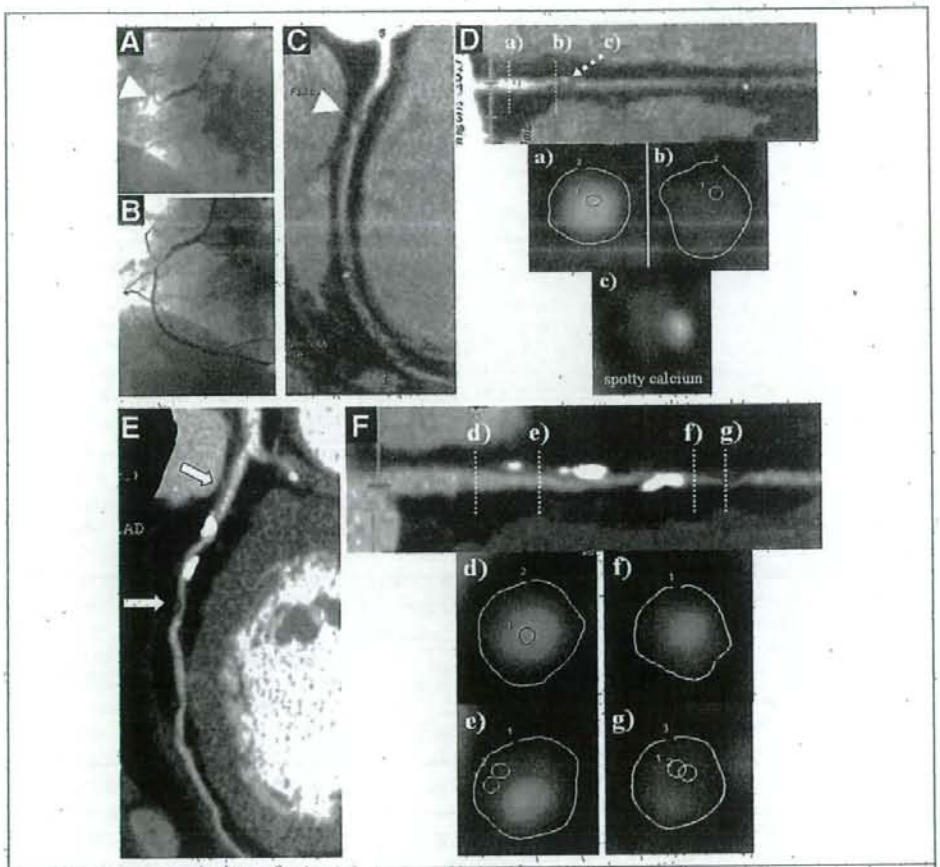

Figure 1. Invasive Angiography and Coronary CT Angiography in a 58-Year-Old Man With NSTEMI

(A and B) Invasive coronary angiographic images show an initial occlusion of the proximal portion of the right coronary artery (RCA) (arrowhead) and a recanalization of the lesion. (C and D) Curved multiplanar reconstruction (MPR) images show the subtotal occlusion and noncalcified coronary atherosclerotic plaque (NCP) with spotty calcium in the proximal portion of the RCA (arrowhead). The cross-sectional vessel areas of the reference site (A) and NCP (B) are 23 and 29 mm^2, respectively. Therefore, the remodeling index (RI) is 1.26. The minimum computed tomography (CT) density of the NCP is 16 Hounsfield units (HU) (B). Spotty calcium with the NCP is observed in the cross-sectional image (C). (E and F) Curved MPR images show multiple nonculprit NCP in left anterior descending coronary artery (LAD) (arrows). The cross-sectional vessel areas of the reference site (D) and nonobstructive NCP (E) in the proximal portion are 28 and 28 mm^2, respectively. Therefore, the RI is 1.0. The minimum CT density of the NCP is 44 HU (E). The cross-sectional vessel areas of the reference site (F) and obstructive NCP (G) in the middle portion are 18 and 18 mm^2, respectively. Therefore, the RI is 1.0. The minimum CT density of the NCP is −7 HU (G). NSTEMI = non–ST-segment elevation myocardial infarction.

accurate discriminator of culprit and nonculprit lesions in ACS patients. Thus, our results provide further evidence for the potential of MDCT angiography to noninvasively identify vulnerable lesions and vulnerable patients.

General findings of NCPs in ACS. In a report using 16-slice CT angiography, the prevalence of noncalcified plaque was 100% in ACS culprit lesions (3). The present study on 64-slice CT also confirms the presence of NCPs in all ACS patients and in all ACS culprit lesions, whereas no patient without any NCP had an ACS. Although the number of ACS patients was small (n = 21), this indicates a high sensitivity of NCP as detected by CT to identify patients with ACS.

Furthermore, our findings are in accordance with previous evidence that the disease process in ACS patients is not focal but more widespread throughout

Table 2. Comparison of NCP Characteristics Between ACS and Non-ACS Groups

	ACS Group (n = 65)	Non-ACS Group (n = 163)	p Value
CT density (HU)			
NCPs (minimum density)	24 ± 22	42 ± 29	< 0.01
Reference site	351 ± 44	357 ± 62	0.46
Remodeling index	1.14 ± 0.18	1.08 ± 0.19	0.02
Adjacent spotty calcium, (n [%])	39 (60)	62 (38)	< 0.01
Low-density NCPs (<40 HU) with PR and spotty calcium, (n [%])	28 (43)	36 (22)	< 0.01

Data are the mean value ± SD or n (%) of non-calcified coronary atherosclerotic plaque (NCPs).
ACS = acute coronary syndrome; CT = computed tomography; HU = Hounsfield units; PR = positive remodeling.

the coronary circulation and might lead to instability of multiple plaques (9). In fact, multiple plaque ruptures in locations other than on the culprit lesion have been detected by IVUS in patients with ACS (10). In the present study, with 64-slice CT angiography that can evaluate the entire coronary tree, more NCPs/patient were detected in the ACS group than the non-ACS group, and those that were detected more frequently displayed "vulnerable" characteristics, such as lower CT density, extent of arterial remodeling, and presence of adjacent spotty calcium. Motoyama et al. (4) reported that 47% of culprit lesions in ACS had all 3 characteristics of PR (RI >1.1), low CT density (<30 HU), and spotty calcium (<3 mm in size). We also observed that 43% of NCPs in the ACS group had all 3 vulnerable characteristics, although the criteria we used varied slightly. This indicates that multiple vulnerable plaques with characteristics similar to the culprit lesion are often present in the entire coronary tree of ACS patients.

Predictors of ACS culprit lesions in MDCT. A previous study with CT angiography (4) revealed that, among the 3 vulnerable characteristics, positive remodeling was the strongest discriminator between culprit and nonculprit lesions in patients with ACS (PR: 87%; low CT density: 79%; spotty calcium: 63%), similar to our results. Whereas this could be explained by previous data, such as a histopathological study using postmortem hearts that revealed that coronary plaques with PR had a higher lipid content and a higher macrophage count (11), or the fact that excessive expansive remodeling promotes continued local lipid accumulation, inflammation, oxidative stress, matrix breakdown, and eventually further plaque progression (12), this observation has to be interpreted with caution. In a retrospective analysis such as ours, the correlation of remodeling and culprit lesions might be a consequence of plaque rupture and not necessarily a predictor. Also, in spite of a significant difference of the mean RI between culprit and nonculprit lesions of ACS patients, the overlap of RI values in these 2 groups was substantial.

Study limitations. Caution is required when interpreting CT densities of NCPs. We cannot exclude the possibility that thrombosis might be present in some ACS culprit lesions, and low-density NCPs are indistinguishable from thromboses due to their similar densities. Thrombosis adjacent to very-low-density NCPs might increase the CT densities that were measured, and this might be 1 of the reasons that the minimum CT density is not statistically different between the culprit and nonculprit lesions in the present study. We believe that selecting the minimum density value as the NCP density is an appropriate method for limiting partial volume and beam hardening effects resulting from neighboring structures, especially hyperdense calcium. However, improvements of spatial resolution will be necessary to more reliably identify and characterize NCPs on the basis of CT densities.

Second, at present, there is no gold standard for determination of coronary plaque vulnerability in CT angiography. For example, in the previous MDCT study, spotty calcium was defined as <3 mm in size (4). However, the visual estimation of high-density structures, such as calcium deposits, varies depending on the window setting in the CT image. Therefore, we believe that our method, which is based on the comparison of calcium dimensions with vessel diameters, is more appropriate for classification of calcium deposits.

Table 3. Comparison of NCP Characteristics Between Culprit and Non-Culprit Lesions in ACS Group

	Culprit Lesions (n = 21)	Non-Culprit Lesions (n = 44)	p Value
CT density (HU)			
NCPs (minimum density)	15 ± 13	28 ± 24	0.07
Reference site	353 ± 46	350 ± 43	0.95
Remodeling index	1.26 ± 0.16	1.09 ± 0.17	< 0.01
Adjacent spotty calcium, (n [%])	12 (57)	27 (61)	0.75
Low-density NCPs (<40 HU) with PR and spotty calcium, (n [%])	12 (57)	16 (36)	0.11

Data are the mean value ± SD or n (%) of NCPs.
Abbreviations as Table 2.

Third, the present study is retrospectively designed, and we assume that vulnerable NCPs have morphological characteristics similar to those of already-disrupted NCPs—a limitation shared with previous studies in this field. A long-term, large prospective trial would be necessary to determine whether CT stratification of NCPs indeed has prognostic value for predicting future cardiac events. Future approaches might, in fact, extend beyond CT analysis of plaque morphology, such as demonstrated by a recent report that described the use of a dedicated contrast agent to visualize macrophage infiltration in atherosclerotic plaques (13).

Finally, our data acquisition protocol led to a relatively high radiation dose for coronary CT angiography. Recently, a prospectively ECG-triggered algorithm has been developed that allows imaging with substantially reduced dose (14). Further studies will be required to validate the accuracy for identification and characterization of NCPs with newer low-dose algorithms.

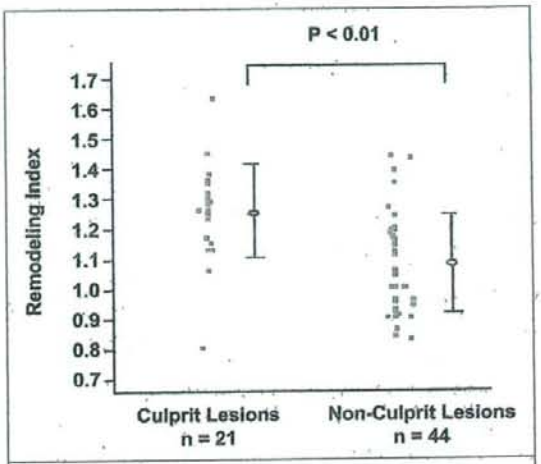

Figure 2. Comparison of RI Between ACS Culprit and Nonculprit Lesions

The mean RI of the culprit lesions is significantly higher than that of the non-culprit lesions (1.26 ± 0.16 vs. 1.09 ± 0.17, $p < 0.01$), but there is a substantial overlap of the distribution of RI values in these 2 groups of lesions. ACS = acute coronary syndrome; RI = remodeling index.

CONCLUSIONS

We were able to demonstrate that 64-slice coronary CT angiography detects a higher number of atherosclerotic lesions with noncalcified components in patients with ACS as compared with patients with stable symptoms. Identifying the actual culprit lesion in ACS patients is more difficult: among the characteristics that are assumed to be associated with plaque "vulnerability" in CT, a large degree of positive remodeling was the only independent predictor of culprit lesions in ACS patients, but a large variability was observed concerning the extent of positive remodeling in culprit and nonculprit lesions. Rather than identifying a single lesion responsible for a future coronary event, the ability to investigate plaque characteristics throughout the entire coronary system in a noninvasive fashion might be an important property of coronary CT angiography regarding its potential application in the context of identifying "vulnerable patients" at risk for ACS.

Acknowledgments

The authors are grateful to Nobuhiko Hirai, MD, and Masao Kiguchi, RT, for their technical assistance. The authors also thank Dr. Shozo Miki for his critical reading of the manuscript.

Reprint requests and correspondence: Dr. Hideya Yamamoto, Department of Cardiovascular Medicine, Graduate School of Biomedical Sciences, Hiroshima University, 1-2-3 Kasumi Minami-ku, Hiroshima 734-8551, Japan. *E-mail: hideyama@hiroshima-u.ac.jp.*

REFERENCES

1. Hausleiter J, Meyer T, Hadamitzky M, et al. Prevalence of noncalcified coronary plaques by 64-slice computed tomography in patients with an intermediate risk for significant coronary artery disease. J Am Coll Cardiol 2006;46:312–8.
2. Butler J, Shapiro M, Reiber J, et al. Extent and distribution of coronary artery disease: A comparative study of invasive versus noninvasive angiography with computed tomography. Am Heart J 2007;153:378–84.
3. Hoffmann U, Moselewski F, Nieman K, et al. Noninvasive assessment of plaque morphology and composition in culprit and stable lesions in acute coronary syndrome and stable lesions in stable angina by multidetector computed tomography. J Am Coll Cardiol 2006;47:1655–62.
4. Motoyama S, Kondo T, Sarai M, et al. Multislice computed tomographic characteristics of coronary lesions in acute coronary syndromes. J Am Coll Cardiol 2007;50:319–26.
5. Kitagawa T, Yamamoto H, Ohhashi N, et al. Comprehensive evaluation of noncalcified coronary plaque characteristics detected using 64-slice computed tomography in patients with proven or suspected coronary artery disease. Am Heart J 2007;154:1191–8.
6. Braunwald E, Antman EM, Beasley JW, et al. ACC/AHA 2002 guideline update for the management of patients with unstable angina and non–ST-segment elevation myocardial infarction–summary article: a report of the American College of Cardiology/American Heart Association Task Force on Practice Guidelines (Committee on the Management of Patients With Unstable Angina). J Am Coll Cardiol 2002;40:1366–74.

7. Achenbach S, Ropers D, Hoffmann U, et al. Assessment of coronary remodeling in stenotic and nonstenotic coronary atherosclerotic lesions by multidetector spiral computed tomography. J Am Coll Cardiol 2004;43:842–7.
8. Kajinami K, Seki H, Takekoshi N, et al. Coronary calcification and coronary atherosclerosis: site by site comparative morphologic study of electron beam computed tomography and coronary angiography. J Am Coll Cardiol 1997;29:1549–56.
9. Buffon A, Biasucci LM, Liuzzo G, et al. Widespread coronary inflammation in unstable angina. N Eng J Med 2002;347:5–12.
10. Rioufol G, Finet G, Ginon I, et al. Multiple atherosclerotic plaque rupture in acute coronary syndrome: a three-vessel intravascular ultrasound study. Circulation 2002;106:804–8.
11. Varnava AM, Mills PG, Davies MJ. Relationship between coronary artery remodeling and plaque vulnerability. Circulation 2002;105:939–43.
12. Chatzizisis YS, Coskun AU, Jonas M, Edelman ER, Feldman CL, Stone PH. Role of endothelial shear stress in the natural history of coronary atherosclerosis and vascular remodeling: molecular, cellular, and vascular behavior. J Am Coll Cardiol 2007;49:2379–93.
13. Hyafil F, Cornily JC, Feig JE, et al. Noninvasive detection of macrophages using a nanoparticulate contrast agent for computed tomography. Nat Med 2007;13:636–41.
14. Earls JP, Berman EL, Urban BA, et al. Prospectively gated transverse coronary CT angiography versus retrospectively gated helical technique: improved image quality and reduced radiation dose. Radiology 2008;246:742–53.

Key Words: acute coronary syndrome ■ multidetector computed tomography ■ noncalcified coronary plaque.

ATH-10383; No. of Pages 8

ELSEVIER

Atherosclerosis xxx (2008) xxx–xxx

ATHEROSCLEROSIS

www.elsevier.com/locate/atherosclerosis

Visceral fat accumulation as a predictor of coronary artery calcium as assessed by multislice computed tomography in Japanese patients

Norihiko Ohashi [a], Hideya Yamamoto [a,*], Jun Horiguchi [b], Toshiro Kitagawa [a], Nobuhiko Hirai [b], Katsuhide Ito [b], Nobuoki Kohno [a]

[a] *Department of Molecular and Internal Medicine, Graduate School of Biomedical Sciences, Hiroshima University, 1-2-3 Kasumi Minami-ku, Hiroshima 734-8551, Japan*

[b] *Department of Radiology, Graduate School of Biomedical Sciences, Hiroshima University, Hiroshima, Japan*

Received 19 January 2008; received in revised form 17 April 2008; accepted 19 April 2008

Abstract

The impact of visceral adiposity on subclinical coronary atherosclerosis is unclear in Japanese patients. We investigated the sex-specific relationship between the amount of visceral fat and coronary artery calcium (CAC) using multislice computed tomography (MSCT). This is a cross-sectional study of 321 consecutive Japanese patients (213 men and 108 women) who underwent MSCT scanning for the examination of coronary heart disease. CAC score, visceral fat area (VFA), subcutaneous fat area (SFA), and waist circumference (WC) were determined by MSCT for all patients. The prevalence of detectable CAC was 73% and 57% in men and women, respectively. Using a multivariable logistic and ordinal regression analyses adjusting for traditional cardiovascular risk factors and adiposity measurements, VFA represented an independent predictor of the presence and extent of CAC (odds ratio (95% confidence interval) per one-unit-standard deviation increase in VFA; 2.48 (1.23–6.05) in logistic regression analysis; 2.05 (1.18–3.98) in ordinal regression analysis). Similar relationships were observed across the gender. We further assessed the sex-specific cut-off levels of VFA and WC to predict the presence of CAC. The results of receiver operator characteristic analysis indicated that the VFA cut-off level in men was 116 cm^2; and in women, it was 82 cm^2, corresponding to WC values of 87.7 cm in men and 82.6 cm in women. In conclusion, we found that visceral adiposity measured by MSCT is significantly associated with the presence and extent of CAC as a marker of subclinical atherosclerosis in Japanese patients.

Keywords: Visceral fat; Coronary calcification; Multislice computed tomography

1. Introduction

Numerous studies have demonstrated the relationship of obesity with the increased risks of coronary heart disease [1,2]. In the past decades, visceral adiposity has been found to be related to a number of atherogenic conditions [3], and it is considered as a part of 'metabolic syndrome'. Excessive accumulation of visceral fat is associated with insulin resistance which contributes to the progression of atherosclerosis [4]. Although several studies have suggested that visceral adiposity may be a stronger predictor of coronary heart disease than overall obesity [5,6], epidemiologic studies of the association among visceral adiposity, overall obesity, and coronary heart disease are still lacking in Japanese populations. Coronary artery calcium (CAC) is considered to be a marker of subclinical atherosclerosis. Many studies using electron-beam tomography have suggested that the presence and extent of CAC strongly correlates with the overall atherosclerotic plaque burden, and with the development of subsequent coronary events [7,8]. Recently, multislice computed tomography (MSCT) has become available, allowing for the reliable detection and quantification of CAC with a high agreement with electron-beam tomography [9,10].

To the best of our knowledge, there has been little research on the relation between visceral adiposity and subclinical atherosclerotic vascular disease in Japanese populations.

* Corresponding author. Tel.: +81 82 257 5197; fax: +81 82 255 7360.
E-mail address: hideyayama@hiroshima-u.ac.jp (H. Yamamoto).

0021-9150/$ – see front matter © 2008 Elsevier Ireland Ltd. All rights reserved.
doi:10.1016/j.atherosclerosis.2008.04.019

Please cite this article in press as: Ohashi N, et al., Visceral fat accumulation as a predictor of coronary artery calcium as assessed by multislice computed tomography in Japanese patients, Atherosclerosis (2008), doi:10.1016/j.atherosclerosis.2008.04.019

Visceral fat area (VFA) measured by CT which is considered as the gold-standard method for determining the quantity of visceral adipose tissues, is a direct index of visceral adiposity [11]. The purpose of this study was to investigate whether body mass index (BMI) and CT measurements of adiposity including VFA, subcutaneous fat area (SFA) and waist circumference (WC) were related to the presence and extent of CAC as detected by MSCT in a clinical setting. We further analyzed the sex-specific cut-off points of the amount of visceral fat for predicting the presence of CAC.

2. Methods

2.1. Subjects

Between August 2005 and June 2007, 390 patients aged 36–87 years underwent MSCT scanning for the examination of coronary heart disease at the Hiroshima University Hospital. We selected consecutive 321 patients for this analysis after exclusion of those who had a history of percutaneous coronary intervention ($n=42$) or coronary artery bypass surgery ($n=27$). Two-hundred and thirty nine patients were asymptomatic and came for regular cardiovascular disease evaluation and 82 patients had the test for the examination of chest pain. MSCT measurements of CAC, VFA, SFA, and WC were also determined for each patient. The study protocol was approved by the Ethics committee at Hiroshima University, and written informed consent was obtained from all patients.

2.2. Risk factor assessment

All patients provided details of their demographics, medical history, and medication usage at the clinical consultation. If a subject was a current smoker, he was considered to have a positive history of cigarette smoking. Patients were classified as hypertensive if their systolic blood pressure was ≥140 mm Hg, diastolic blood pressure was ≥90 mm Hg, and/or the subject was on antihypertensive therapy. Prior to CT scan, we obtained fasting blood samples from an antecubital vein. Concentrations of triglycerides and uric acid were measured with standard enzymatic methods. High-density lipoprotein (HDL) cholesterol and low-density lipoprotein (LDL) cholesterol were measured by direct methods. Glycohemoglobin A1c (HbA1c) was measured using high-performance liquid chromatography. Diabetes mellitus was defined by self-report and current use of hypoglycemic agents. Hypercholesterolemia was characterized by a fasting serum LDL cholesterol level ≥ 140 mg/dl on direct measurement [12], or when the patient was using lipid-lowering agents. Metabolic syndrome was diagnosed by Japanese criteria, which was reported in 2005 [13]. Height (m) and body weight (kg) were used to calculate the body mass index (BMI).

2.3. CAC scoring using MSCT

Total of 321 consecutive patients were imaged using either a 16-slice MSCT scanner (LightSpeed Ultrafast16, GE Healthcare, Waukesha, Wisconsin) between August 2005 and November 2005 (men, 27; women, 17; age 66 ± 10 years) or a 64-slice CT scanner (LightSpeed VCT, GE Healthcare) between December 2005 and June 2007 (men, 186; women, 91; age 65 ± 11 years). Prospective electrocardiogram-triggered scans were performed in mild inspiration from the root of aorta to the apex of the heart with the following parameters (16-slice CT and 64-slice CT): axial scan; gantry rotation times, 500 ms and 350 ms; X-ray exposure times, 333 ms and 233 ms; tube voltage, 120 kV; tube currents, 100 mA and 140 mA; center of imaging window, 75% of R-R. Thirty-five to 40 contiguous images of 2.5-mm thickness were obtained.

The calcium score was determined using a commercially available external workstation (Advantage Windows, version 4.2, GE Healthcare), and using the CAC scoring software (Smartscore, version 3.5, GE Healthcare). CAC score (CACS) was calculated according to the Agatston method as previously described [14]. We defined the regions of interest based on the vessels and slices, and using the threshold option for pixels greater than 130 Hounsfield units (HU) to measure the area and peak density of the plaques. Depending on the peak density of the plaque, an area of at least 0.52 mm^2 (2 pixels) was multiplied by one of the following cofactors: a factor of one for 130–199 HU, a factor of two for 200–299 HU, a factor of three for 300–399 HU, and a factor of 4 for densities greater than 400 HU. The total coronary artery calcium score was calculated as the sum of the individual lesion scores in all coronary arteries.

2.4. Measurement of VFA, SFA, and WC using MSCT

In addition to MSCT heart scans, abdominal scans were performed at the lumbar 4–5 levels in spine position, and single 5-mm slices were taken during suspended respiration after normal expiration. The fat areas and WC in each subject were determined from an image at the level of the umbilicus using a commercially supplied software (Virtual Place, AZE Inc., Tokyo, Japan). Subcutaneous fat was defined as the extraperitoneal fat between the skin and muscles, with attenuation ranging from −150 to −50 HU. The intraperitoneal part with the same density as the subcutaneous fat layer was defined as visceral fat. The VFA and SFA were determined by automatic planimetry. The WC was determined at the umbilicus level using a mobile caliper.

2.5. Statistical analysis

Categorical variables were presented as number of patients (%) and continuous variables were expressed as mean ± S.D. Between-group comparisons were performed using Student's t-test or the Mann–Whitney U-test and the correlation

Please cite this article in press as: Ohashi N, et al., Visceral fat accumulation as a predictor of coronary artery calcium as assessed by multislice computed tomography in Japanese patients, Atherosclerosis (2008), doi:10.1016/j.atherosclerosis.2008.04.019

coefficient was estimated by Pearson correlation. Differences among three groups by CAC category were tested by ANOVA with post hoc analysis. Multivariable logistic regression analysis was performed to assess the independent relationship of metabolic syndrome and adiposity measurements to the presence of CAC. Additionally, we also used ordinal regression analysis to assess the relationship of metabolic syndrome and adiposity measurements with increasing levels of CAC [15]. Confidence intervals (CI) that excluded 1.0 were considered to indicate significant results. Utilization of CAC scores as a continuous variable in standard parametric analyses is extremely challenging due to high frequency of zero scores resulting in a high skewed distribution, CAC scores were therefore dichotomized (i.e., presence or absence of CAC) for use in logistic regression analysis. We also categorized CAC scores into three groups: 0, 1–100 and >100 for use in ordinal regression analysis. For analysis between metabolic syndrome and CAC, we used a set of atherosclerotic risk factors – age, current smoking, LDL cholesterol, uric acid and lipid-lowering agents – as explanatory variables. Two sets of multivariable models were used in a hierarchical fashion to determine the independent association of the adiposity measurements. Model 1 was adjusted for traditional cardiovascular risk factors including hypertension, diabetes, current smoking, triglycerides, HDL cholesterol, LDL cholesterol, uric acid and HbA1c levels, and medication use. Metabolic syndrome was not included in the model because of collinearity. Model 2 was additionally standardized for fat measurements including VFA, BMI, SFA, and WC. A receiver operator characteristic (ROC) analysis was performed to determine the increase in discriminative ability that was afforded by VFA in addition to clinical fat measurements such as BMI and WC. All analyses were performed on the whole population and then stratified by gender. Furthermore, the sex-specific VFA was tested using a ROC curve to detect the presence of CAC. The optimal cut-off point was obtained from the Youden index (maximum (sensitivity + specificity − 1)) [16]. All analyses were performed using the JMP 5.0.1 statistical software (SAS Institute Inc, North Carolina). A p value < 0.05 was considered statistically significant.

3. Results

3.1. Patient characteristics

The study patients consisted of 213 men (mean age, 65 years; range, 36–87 years) and 108 women (mean age, 68 years; range, 44–86 years). Coronary calcium, defined as CAC > 0, was present in 73% men and 57% women. The median (range) CAC in men and women were 138 (0–4370) and 33.5 (0–1998), respectively. The distribution of CAC by sex is shown in Fig. 1a. The characteristics of the study subjects based on CAC status are shown in Table 1. In both sexes, patients with any CAC were significantly older, had a higher BMI, a larger VFA, SFA, VFA/SFA ratio and WC, and a higher prevalence of hypertension, hypercholesterolemia, diabetes and metabolic syndrome. The percentages of pharmacological treatment for hypertension and diabetes were significantly higher in men with CAC than those without and in hypertensive women with CAC.

3.2. Metabolic syndrome and coronary artery calcium

The prevalence of metabolic syndrome in our study patients was 41.4% (133/321) in all subjects, 49.8% (106/213) in men and 25.0% (27/108) in women. Multivariable logistic regression analysis showed that the odds ratio of the presence of CAC, adjusted for age, sex (for all subjects), current smoking, uric acid, LDL cholesterol and lipid-lowering agents, was 4.28 (95%CI, 2.14–9.02; $p < 0.0001$) in all subjects, 3.83 (95%CI, 1.61–9.81; $p = 0.0032$) in men and 5.23 (95%CI, 1.65–20.7; $p = 0.0088$) in women. Similarly, multivariable ordinal regression analysis revealed that the odds ratio of increasing CAC categories, adjusted for the same explanatory variables as above, was 1.71 (95%CI, 1.31–2.25; $p < 0.0001$) in all subjects, 1.66 (95%CI, 1.19–2.33; $p = 0.0030$) in men and 1.93 (95%CI, 1.21–3.16; $p = 0.0064$) in women. These results demonstrated that metabolic syndrome was an independent predictor of CAC in both sexes.

3.3. Adiposity measurements and coronary artery calcium

Adiposity measurements were all significantly correlated with each other, as shown in Table 2. VFA was strongly correlated with WC ($r = 0.79$) and moderately correlated with BMI ($r = 0.51$) and SFA ($r = 0.44$). Fig. 1b shows the mean adiposity measurements (VFA, BMI and SFA) according to the CAC category in both sexes. In men, VFA and BMI were significantly different between the CAC: 0 and CAC: >400 groups ($p < 0.0001$ and $p = 0.001$), whereas SFA was significantly lower in the CAC: >400 group compared with the CAC: 101–400 group ($p = 0.04$). In women, VFA, BMI and SFA were all significantly different between the CAC: 0 and CAC: >400 groups ($p < 0.0001$, $p < 0.0001$, $p = 0.0012$).

Table 3 describes the association of adiposity measurements with CAC using multivariable logistic and ordinal regression analysis. As for all subjects, in Model 1 adjusting for age and traditional risk factors, the odds ratio (95%CI) of the presence of CAC for one-unit-standard deviation increase in VFA (69.8 cm^2), BMI (3.1 kg/m^2) and WC (9.5 cm) were 2.01 (1.32–3.27), 1.41 (1.01–1.98) and 1.61 (1.10–1.98), respectively. Similarly, the association of VFA, BMI and WC with increasing CAC categories in the ordinal regression analysis was also statistically significant. On the other hand, both SFA and VFA/SFA ratio (data not shown) were not significantly associated with CAC. In Model 2, which additionally standardized for VFA, BMI, SFA and WC, only VFA persisted to show a significant relationship with CAC in both

Please cite this article in press as: Ohashi N, et al., Visceral fat accumulation as a predictor of coronary artery calcium as assessed by multislice computed tomography in Japanese patients, Atherosclerosis (2008), doi:10.1016/j.atherosclerosis.2008.04.019

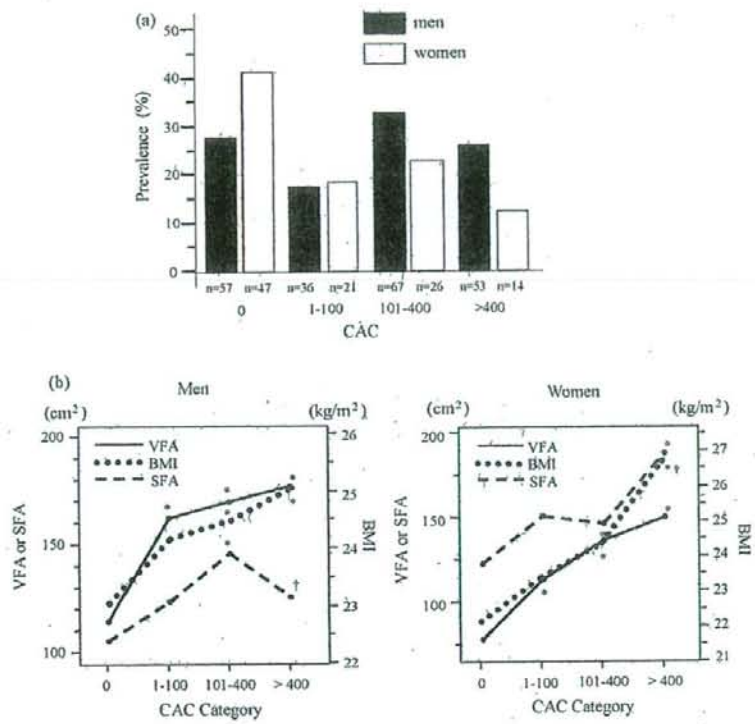

Fig. 1. (a) Distribution of multislice computed tomography (MSCT)-derived coronary artery calcium score by sex. Solid bars and open bars represent men and women, respectively. (b) Mean fat measurements according to the coronary artery calcium (CAC) category in men and women. Solid lines, dotted lines, and broken lines denote visceral fat area (VFA), body mass index (BMI) and subcutaneous fat area (SFA), respectively. Mean values of fat measurements for CAC category: 0, 1–100, 101–400, >400 are 115, 162, 170, 177 cm^2 for VFA, 23.1, 24.1, 24.4, 24.9 kg/m^2 for BMI and 106, 124, 146, 125 cm^2 for SFA in men and 80, 115, 138, 152 cm^2 for VFA, 22.3, 23.5, 24.4, 26.6 kg/m^2 for BMI and 124, 153, 148, 189 cm^2 for SFA in women, respectively. $^*p < 0.01$ versus CAC: 0, $^\dagger p < 0.05$ versus CAC: 101–400.

logistic and ordinal regression analyses and was regarded as an independent determinant of CAC. Similar relationships were observed across the gender except that BMI was not associated with CAC in men.

On ROC analysis in all subjects, the area under the curve (AUC) for clinical variables including BMI and WC for presence of CAC > 0 and significant CAC > 100 were 0.740 and 0.698, respectively. When VFA was added in the model, AUC improved to 0.785 and 0.726, respectively. Similar results were obtained for men and women.

3.4. Sex-specific cut-off levels of VFA and WC to predict the presence of CAC

From the ROC curve analysis, the optimal cut-off value of VFA to predict the presence of CAC was identified as 116 cm^2 in men, and 82 cm^2 in women. These values provided sensitivities of 79% and 84%, and specificities of 63% and 72% for men and women, respectively (Fig. 2A). Fig. 2B shows the sex-specific correlation between the measured values of VFA and WC using MSCT. According to the regression equations, the VFA cut-off values corresponded with WC of 87.7 cm and 82.6 cm in men and women, respectively.

4. Discussion

To the best of our knowledge, this is the first study to investigate the sex-specific relationship between visceral adiposity measured by MSCT and the presence and extent of CAC in Japanese patients. VFA, a direct index of visceral adiposity, was found to be an independent predictor of the presence and quantity of CAC even after adjustment for BMI, SFA, WC, age, and traditional cardiovascular risk factors in both sexes. These results are consistent with the accumulating evidence that measurements of visceral adiposity are more strongly related to cardiovascular disease compared with BMI [5,6]. We further assessed the sex-specific cut-off levels of VFA and WC to predict the presence of CAC. The results of the ROC analysis indicated that the VFA cut-off levels were 116 and 82 cm^2 in men and women, respectively, which corresponded to WC

Please cite this article in press as: Ohashi N, et al., Visceral fat accumulation as a predictor of coronary artery calcium as assessed by multislice computed tomography in Japanese patients, Atherosclerosis (2008), doi:10.1016/j.atherosclerosis.2008.04.019

Table 1
Patient characteristics according to CAC status

	All subjects ($n=321$)		Men ($n=213$)		Women ($n=108$)	
	No CAC ($n=104$)	Any CAC ($n=217$)	No CAC ($n=57$)	Any CAC ($n=156$)	No CAC ($n=47$)	Any CAC ($n=61$)
Age (yrs)	62 ± 12	68 ± 9**	60 ± 13	67 ± 9**	65 ± 9	71 ± 7**
BMI (kg/m^2)	22.7 ± 3.1	24.5 ± 2.9**	23.1 ± 2.9	24.5 ± 2.8**	22.3 ± 3.4	24.6 ± 3.1**
Hypertension, *n* (%)	34 (33)	139 (64)**	19 (33)	99 (64)**	15 (32)	40 (66)**
Hypercholesterolemia, *n* (%)	35 (34)	133 (61)**	18 (32)	93 (60)**	17 (36)	40 (66)**
Diabetes mellitus, *n* (%)	34 (33)	122 (56)**	16 (28)	85 (55)**	18 (38)	37 (61)*
Current Smoking, *n* (%)	29 (28)	94 (43)**	23 (40)	84 (54)*	6 (13)	10 (16)
Metabolic syndrome, *n* (%)	19 (18)	114 (53)**	15 (26)	91 (58)**	4 (9)	23 (38)**
Triglyceride (mg/dl)	128 ± 65.5	163 ± 84.7**	132 ± 71.1	164 ± 85.0*	124 ± 58.5	159 ± 84.7*
HDL cholesterol (mg/dl)	60.4 ± 19.4	51.9 ± 16.5**	59.1 ± 22.7	49.9 ± 15.7**	62.0 ± 14.5	57.0 ± 17.5*
LDL cholesterol (mg/dl)	112 ± 28.4	125 ± 33.4**	109 ± 27.7	123 ± 35.5**	114 ± 29.2	130 ± 29.1**
HbA1c (%)	5.9 ± 1.0	6.5 ± 1.2**	5.9 ± 1.1	6.4 ± 1.2**	5.9 ± 1.0	6.7 ± 1.1**
Uric acid (mg/dl)	5.5 ± 1.6	5.9 ± 1.3**	5.8 ± 1.9	6.2 ± 1.3	5.2 ± 1.2	5.4 ± 1.2
VFA (cm^2)	99 ± 59.8	160 ± 65.6**	115 ± 67.0	170 ± 67.6**	80 ± 43.4	133 ± 52.0**
SFA (cm^2)	114 ± 65.5	141 ± 55.8**	106 ± 58.6	134 ± 53.2**	125 ± 72.3	159 ± 58.5**
V/S ratio	1.09 ± 1.11	1.24 ± 0.50**	1.26 ± 0.90	1.37 ± 0.50**	0.72 ± 0.37	0.89 ± 0.32**
WC (cm^2)	84.6 ± 10.1	92.3 ± 8.1**	86.3 ± 1.1	93.5 ± 0.7**	82.5 ± 9.3	89.4 ± 8.1**
Medication						
Antihypertensive agents, *n* (%)	14 (13)	67 (31)**	8 (14)	48 (31)*	6 (13)	19 (31)*
Lipid-lowering agents, *n* (%)	25 (24)	76 (35)*	13 (23)	55 (35)	12 (26)	21 (34)
Hypoglycemic agents, *n* (%)	26 (25)	62 (29)	8 (14)	42 (27)*	18 (38)	20 (33)

*$p<0.05$, **$p<0.001$. All data are presented as number of patients (%) or mean ± S.D. CAC, coronary artery calcium; BMI, body mass index; HDL, high-density lipoprotein; LDL, low-density lipoprotein; HbA1c, glycohemoglobin A1c; VFA, visceral fat area; SFA, subcutaneous fat area; V/S ratio, visceral fat area/subcutaneous fat area ratio; WC, waist circumference.

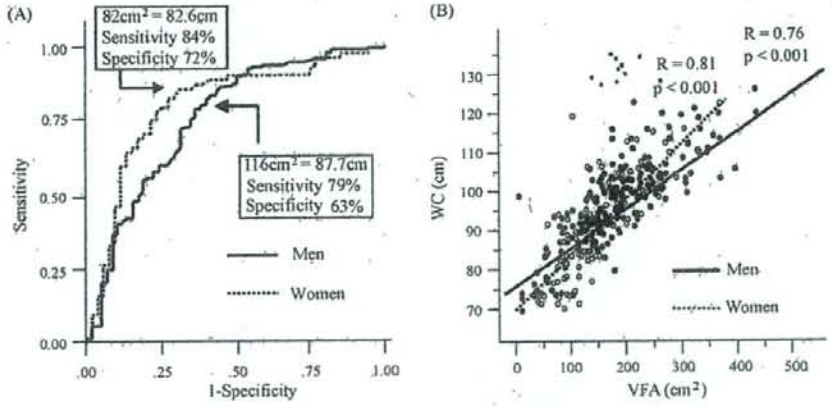

Fig. 2. (A) Receiver operating characteristic (ROC) analysis of the visceral fat area (VFA) to predict the presence of coronary calcium. Solid lines and broken lines depict the ROC curves for men and women, respectively. (B) Correlation between waist circumference (WC) and VFA. Closed circles and open circles indicate the data for men and women, respectively. The solid lines and broken lines represent the men and women, respectively.

values of 87.7 cm and 82.6 cm in men and women, respectively.

Although numerous studies have demonstrated that visceral adiposity is a risk factor for cardiovascular disease, little research has been conducted on the association between visceral adiposity and early atherosclerosis. A number of more recent studies have specifically reported on the effect of excess visceral fat on CAC. In the St. Francis Heart Study, visceral obesity measured by the waist-to-hip ratio or intra-abdominal-fat was positively correlated with CAC

Table 2
Age- and sex-adjusted Pearson correlation coefficients*

	VFA	SFA	BMI	WC
VFA	1	0.44	0.51	0.79
SFA	0.44	1	0.6	0.61
BMI	0.51	0.6	1	0.59
WC	0.79	0.61	0.59	1

* $p<0.001$ for all correlations.

Please cite this article in press as: Ohashi N, et al., Visceral fat accumulation as a predictor of coronary artery calcium as assessed by multislice computed tomography in Japanese patients, Atherosclerosis (2008), doi:10.1016/j.atherosclerosis.2008.04.019

Table 3
Multivariable analysis of the association between adiposity measurement and coronary artery calcium

	Multivariable logistic regression analysis[a]					
	All subjects ($n=321$)		Men ($n=213$)		Women ($n=108$)	
	Odds ratio (95%CI[b])	p value	Odds ratio (95%CI[b])	p value	Odds ratio (95%CI[b])	p value
Model 1[c]						
VFA (cm^2)	2.01 (1.32–3.27)	0.002	2.37 (1.32–4.53)	0.006	3.70 (1.56–10.1)	0.006
BMI (kg/m^2)	1.41 (1.01–1.98)	0.04	1.53 (0.98–2.46)	0.06	1.82 (1.03–3.39)	0.04
SFA (cm^2)	1.27 (0.94–1.82)	0.1	1.60 (0.96–2.76)	0.08	1.67 (0.97–3.01)	0.07
WC (cm)	1.61 (1.10–1.98)	0.01	1.97 (1.17–3.52)	0.02	1.83 (1.00–3.54)	0.05
Model 2[d]						
VFA (cm^2)	2.48 (1.23–6.05)	0.02	5.06 (1.14–16.4)	0.04	3.90 (1.26–14.4)	0.02
BMI (kg/m^2)	1.23 (0.79–1.92)	0.4	1.17 (0.63–2.17)	0.6	1.20 (0.51–2.97)	0.6
SFA (cm^2)	0.74 (0.38–1.27)	0.3	0.43 (0.12–1.55)	0.2	1.40 (0.57–3.57)	0.4
WC (cm)	1.01 (0.52–1.98)	0.9	1.20 (0.46–3.23)	0.7	0.64 (0.20–1.97)	0.4
	Multivariable ordinal regression analysis[e]					
Model 1[c]						
VFA (cm^2)	1.82 (1.29–2.60)	0.001	1.64 (1.14–2.44)	0.008	2.85 (1.44–6.18)	0.003
BMI (kg/m^2)	1.37 (1.05–1.82)	0.02	1.27 (0.93–1.75)	0.1	1.88 (1.12–3.26)	0.02
SFA (cm^2)	1.29 (0.81–1.71)	0.07	1.36 (0.97–1.93)	0.07	1.55 (0.95–2.62)	0.07
WC (cm)	1.55 (1.13–2.15)	0.006	1.44 (1.02–2.06)	0.04	1.86 (1.09–3.32)	0.02
Model 2[d]						
VFA (cm^2)	2.05 (1.18–3.98)	0.02	2.08 (1.05–4.90)	0.05	2.67 (1.66–7.37)	0.04
BMI (kg/m^2)	1.16 (0.81–1.67)	0.4	1.04 (0.70–1.56)	0.8	1.40 (0.67–3.00)	0.4
SFA (cm^2)	0.81 (0.49–1.29)	0.4	0.82 (0.39–1.53)	0.5	1.17 (0.57–2.44)	0.7
WC (cm)	1.03 (0.61–1.75)	0.9	0.98 (0.55–1.77)	0.9	0.78 (0.29–2.06)	0.6

[a] The results of logistic regression analysis are presented as the odds ratio of the presence of CAC for one-unit-standard deviation increase in adiposity measurement.

[b] 95% confidence interval.

[c] Adjusted for age, hypertension, diabetes, smoking status, triglycerides, LDL cholesterol, HDL cholesterol, HbA1c, uric acid and medication use. Abbreviations are the same as in Table 1.

[d] Model 1 plus adjustment for VFA, BMI, SFA or WC. Abbreviations are the same as in Table 1.

[e] The results of ordinal regression analysis are presented as the odds ratio of increasing CAC category (0, 1–100 and >100) for one-unit-standard deviation increase in adiposity measurement.

in 50–70-years-old US men and women [17]. The recent CARDIA study has demonstrated that abdominal obesity measured by waist girth or waist-to-hip ratio is associated with CAC in African American and White young adults [18]. With respect to obesity and CAC in diabetic individuals, the PREDICT study showed that the waist-to-hip ratio was a significant predictor of CAC after adjustment for multiple cardiovascular risk factors in 495 diabetic subjects [19]. In another multiethnic study on type 2 diabetes, visceral fat measured by CT predicted CAC [20]. These results support our findings, i.e., visceral fat measured directly using MSCT is an independent predictor of CAC in Japanese patients, in the daily clinical practice.

The distribution of body fat has been focused as a cardiovascular risk. Interestingly, in our study, SFA was lower in men with significant CAC > 400, which raises the possibility that the increasing subcutaneous fat has a favorable effect on atherosclerosis. This finding is relevant as peripheral fat such as subcutaneous or gluteal fat has been shown to be protective against cardiovascular and metabolic outcomes [3,6]. However, more definitive studies will be necessary to validate this hypothesis. Recently, a study from the Framingham Heart Study has shown that pericardial fat, which is an ectopic fat depot around the heart, is more associated with CAC than visceral fat [21]. It is interesting because the result of this study suggested that pericardial fat may potentially exert local atherosclerotic effects due to anatomical close proximity to the coronary arteries. Further investigation is needed to determine if this finding is true as well as our patient-based sample study.

Several prior studies have identified some plausible mechanisms by which the accumulation of visceral fat could directly accelerate atherosclerosis [4]. It is generally assumed that insulin resistance is one of the most important factors linking visceral fat to the clustering of cardiovascular risk factors. Insulin resistance has also been postulated to be largely responsible for endothelial dysfunction, platelet activation, and the progression of atherosclerosis [22,23]. Visceral adiposity is also associated with increased levels of proinflammatory cytokines like tumor necrosis factor-alpha (TNF-α), and interleukin-6 (IL-6), and less adiponectin. These cytokines are suggested to induce insulin resistance, and play a major role in the pathogenesis of endothelial dysfunction and subsequent atherosclerosis [24,25].

CAC is a marker of atherosclerosis that can be quantified by using MSCT, and it is proportional to the extent and

Please cite this article in press as: Ohashi N, et al., Visceral fat accumulation as a predictor of coronary artery calcium as assessed by multislice computed tomography in Japanese patients, Atherosclerosis (2008), doi:10.1016/j.atherosclerosis.2008.04.019

severity of atherosclerotic disease. In previous large studies, an increased plaque burden was found to be a significant predictor of future cardiovascular events and mortality in symptomatic and asymptomatic subjects [7,8]. The detection and quantification of CAC by MSCT could potentially provide a preventive strategy for cardiovascular events. There is ample evidence demonstrating that individuals with visceral adiposity represent a population at high risk for the progression of atherosclerosis and cardiovascular events. Cassidy et al. reported that several indices of adiposity measurements including waist circumference and waist-to-hip ratio predicted the progression of CAC in patients with a low risk for cardiovascular disease [26]. The strong association between increased amount of visceral fat and quantity of CAC observed in our study could explain, at least in part, the excess risk of atherosclerosis in abdominal obese patients. Therefore, measuring visceral fat is a useful clinical tool for identifying patients with potential future cardiovascular disease risk. Furthermore, our study may still add to the knowledge suggesting that the presence of higher VFA will have a rapid progression of CAC and may still need more aggressive risk modification even if the CAC scores are same across different patients. Considering the cross-sectional nature of this study, causality cannot be established. Ultimately, a trial that specifically focuses on weight reduction and decreases in visceral fat amount would verify a possible causal relationship between visceral adiposity and atherosclerosis.

In the latest Japanese criteria [13], visceral adiposity is a requisite factor in metabolic syndrome. Men and women with a waist circumference greater than 85 cm and 90 cm, respectively, are considered to have an increased risk for more than one obesity-related disease (i.e., hyperglycemia, hypertension, dyslipidemia, hyperuricemia, and cardiovascular disease). These cut-off points were derived from a regression curve that identified the WC values corresponding to a VFA of 100 cm^2. However, several studies revealed a gender difference in the association of visceral fat accumulation with metabolic syndrome. Hayashi et al. analyzed data from 639 Japanese Americans, and reported that the optimal cut-off points for VFA and WC to predict metabolic syndrome were 96.1 cm^2 and 87.1 cm in men (age, >57years); and 86.3 cm^2 and 89.0 cm in women (age, >56 years) [27]. Recently, metabolic syndrome has been found to be associated with endothelial dysfunction, a hallmark of early atherosclerotic changes, coronary calcification, and subclinical atherosclerosis of the carotid artery [28,29]. Our study has demonstrated that metabolic syndrome is an independent predictor of CAC, which is consistent with the prior finding [28].

This study had some limitations. First, data were exclusively collected from middle-aged and older Japanese patients with a high risk for cardiovascular disease in a single institute using a retrospective method. As a result, it is uncertain whether our findings can be generalized to other ethnic groups or healthy young subjects. Prospective and non-randomized investigations should be warranted. Second, we used the CT-measured WC value when calculating the WC cut-off, though anthropometric measured WC values are currently used for the diagnosis of visceral obesity for metabolic syndrome. The relationship between CT and the anthropometric measured WC should be confirmed in Japanese populations. Third, we could not evaluate the relationship between CAC and other confounding factors including inflammatory mediators and adipocytokines, which may not allow us to exclude the potential effects of these influences on CAC. Fourth, although we used 16- and late 64-slice CT to measure CAC, accuracy comparison of both methods could not be evaluated. Horiguchi et al. reported that the sensitivity and specificity in the detection of CAC using 16-slice CT with a threshold of 130 HU were 98.7% and 100%, respectively [30]. Further investigation of the interscanner variability of CAC measurement is needed.

5. Conclusions

We found that visceral adiposity measured by MSCT is significantly associated with the presence and extent of CAC in Japanese patients. Follow-up studies are needed to examine the influence of greater visceral fat accumulation on the development of new calcification or the progression of CAC scores.

References

[1] Manson JE, Colditz GA, Stampfer MJ, et al. A prospective study of obesity and risk of coronary heart disease in women. N Engl J Med 1990;322:882–9.
[2] Wilson PW, D'Agostino RB, Sullivan L, Parise H, Kannel WB. Overweight and obesity as determinants of cardiovascular risk: the Framingham experience. Arch Intern Med 2002;162:1867–72.
[3] Goodpaster BH, Krishnaswami S, Harris TB, et al. Obesity, regional body fat distribution, and the metabolic syndrome in older men and women. Arch Intern Med 2005;165:777–83.
[4] Van Gaal LF, Mertens IL, De Block CE. Mechanisms linking obesity with cardiovascular disease. Nature 2006;444:875–80.
[5] See R, Abdullah SM, McGuire DK, et al. The association of differing measures of overweight and obesity with prevalent atherosclerosis: the Dallas Heart Study. J Am Coll Cardiol 2007;50:752–9.
[6] Yusuf S, Hawken S, Ounpuu S, et al. Obesity and the risk of myocardial infarction in 27,000 participants from 52 countries: a case-control study. Lancet 2005;366:1640–9.
[7] LaMonte MJ, FitzGerald SJ, Church TS, et al. Coronary artery calcium score and coronary heart disease events in a large cohort of asymptomatic men and women. Am J Epidemiol 2005;162:421–9.
[8] Budoff MJ, Shaw LJ, Liu ST, et al. Long-term prognosis associated with coronary calcification: observations from a registry of 25,253 patients. J Am Coll Cardiol 2007;49:1860–70.
[9] Detrano RC, Anderson M, Nelson J, et al. Coronary calcium measurements: effect of CT scanner type and calcium measure on rescan reproducibility—MESA study. Radiology 2005;236:477–84.
[10] Horiguchi J, Shen Y, Akiyama Y, et al. Electron beam CT versus 16-MDCT on the variability of repeated coronary artery calcium measurements in a variable heart rate phantom. AJR Am J Roentgenol 2005;185:995–1000.

Please cite this article in press as: Ohashi N, et al., Visceral fat accumulation as a predictor of coronary artery calcium as assessed by multislice computed tomography in Japanese patients, Atherosclerosis (2008), doi:10.1016/j.atherosclerosis.2008.04.019